Effect of polarization on broadband second-harmonic generation in periodically poled lithium tantalate

M. YIN*, Y. GUO, X. ZHONG
College of Information Science & Technology, Chengdu University of Technology, 610059, Chengdu, China

Quasi-phase matching (QPM) broadband second-harmonic generation (SHG) has attracted much attention, however, the effect of polarization on QPM broadband SHG is not clear in periodically poled lithium tantalate (PPLT). In this paper, four QPM types broadband SHGs are studied in PPLT. Group-velocity matching (GVM) fundamental wavelength and SHG bandwidth vary with polarization varying. GVM fundamental wavelength and SHG bandwidth are positively correlated with temperature for some QPM types and negatively for another types. Temperature sensitivity of GVM fundamental wavelength for type Ⅰ is maximum and that for type 0 is minimum. Results can be used in new wavelength broadband SHG.

(Received April 14, 2017; accepted August 9, 2018)

Keywords: Quasi-phase matching, Second-harmonic generation, Broadband, Periodically poled lithium tantalate, Group-velocity matching

1. Introduction

Broadband second-harmonic generation (SHG) is widely used in femtosecond and tunable laser frequency doubling and all optical wavelength conversion. [1,2] As quasi-phase matching(QPM) is more simple and flexible than birefringent-phase matching, QPM broadband SHG has attracted much attention in periodically poled potassium niobate (PPKN) [3,4], periodically poled potassium titanyl phosphate (PPKTP) [5-7], periodically poled lithium niobate (PPLN) [1,2,8-12], periodically poled lithium tantalate (PPLT) [13-16], and orientation-patterned gallium arsenide (OP-GaAs) [17]. For PPLT, effects of temperature and magnesium oxide doping concentration on QPM broadband SHG have been investigated [13,15], however, the effect of polarization on QPM broadband SHG is not clear.

In this paper, four QPM types broadband SHGs are studied in magnesium oxide-doped PPLT. Group-velocity matching (GVM) conditions are derived, GVM fundamental wavelengths and corresponding poling periods are calculated at room temperature (25 °C), effects of temperature on GVM fundamental wavelength and corresponding poling period are analyzed, SHG bandwidths are obtained at room temperature, 100 and 200 °C. Effects of polarization on GVM fundamental wavelength, temperature sensitivity of GVM fundamental wavelength and SHG bandwidth are investigated. The results provide a basis on wavelength range expansion of efficient broadband SHG.

2. Theory analysis

For efficient single wavelength SHG, the wave vector mismatch Δk must fulfill Eq. (1)

$$\Delta k = 0, \tag{1}$$

If efficient broadband SHG is obtained, the wave vector mismatch Δk must fulfill Eq. (2) besides Eq. (1),

$$\frac{d\Delta k}{d\lambda_f} = 0, \tag{2}$$

where λ_f is fundamental wavelength.[8]

For collinear first-order QPM SHG, Δk can be written as [10]

$$\Delta k = \frac{2\pi n_s}{\lambda_s} - \frac{2\pi n_f}{\lambda_f} - \frac{2\pi}{\Lambda}, \tag{3}$$

where n_f is the refractive index of fundamental wave and n_s is the refractive index of second-harmonic wave, λ_f is the fundamental wavelength and λ_s is the second-harmonic wavelength, and Λ is the crystal poling period.

According to polarizations of fundamental and second-harmonic waves, QPM has six types (*o*+*o*-*e*, *o*+*e*-*e*, *o*+*o*-*o*, *e*+*e*-*e*, *o*+*e*-*o* and *e*+*e*-*o*). "*o*" represents ordinary light wave, "*e*" represents extraordinary light

wave, polarizations of ordinary and extraordinary light wave are vertical in one crystal. GVM conditions must be fulfilled in order to obtain efficient broadband SHG. GVM conditions of *o*+*o*-*e* and *e*+*e*-*e* types are derived[10]. From Eq. (2) and (3), GVM conditions of rest types are derived as

for *o*+*e*-*e*

$$\frac{1}{v_{fo}}+\frac{1}{v_{fe}}=\frac{2}{v_{se}}, \tag{4}$$

for *o*+*o*-*o*

$$\frac{1}{v_{fo}}=\frac{1}{v_{so}}, \tag{5}$$

for *o*+*e*-*o*

$$\frac{1}{v_{fo}}+\frac{1}{v_{fe}}=\frac{2}{v_{so}}, \tag{6}$$

for *e*+*e*-*o*

$$\frac{1}{v_{fe}}=\frac{1}{v_{so}}, \tag{7}$$

where v_{fo} is the group velocity of fundamental ordinary light wave, v_{fe} is the group velocity of fundamental extraordinary light wave, v_{se} is the group velocity of second-harmonic extraordinary light wave, and v_{so} is the group velocity of second-harmonic ordinary light wave.

The Sellmeier equation of magnesium oxide-doped PPLT can be obtained from [18]. The length of PPLT is assumed to be 10 mm for the simulation.

3. Results

For *o*+*e*-*e* type QPM, $\frac{d\Delta k}{d\lambda_f}$ and QPM Λ are calculated as a function of λ_f at room temperature, as shown in Fig. 1 (a). $\frac{d\Delta k}{d\lambda_f}$ equals zero at 2.536 μm, the fundamental wavelength which makes $\frac{d\Delta k}{d\lambda_f}$ equal zero is GVM λ_f, the GVM λ_f is 2.536 μm at room temperature for *o*+*e*-*e* type QPM. From Eq. (1) and (3), it can be seen that every fundamental wavelength corresponds a poling period which make fundamental and second-harmonic waves fulfill QPM condition, this poling period is QPM Λ. The QPM Λ is 35.62 μm at 2.536 μm. QPM broadband SHG can be realized near 2.536 μm with Λ 35.62 μm for *o*+*e*-*e* type. The dependence of temperature on GVM λ_f and corresponding QPM Λ is shown in Fig. 1 (b). The GVM λ_f increases from 2.536 to 2.650 μm and corresponding QPM Λ decreases from 35.62 to 31.55 μm with temperature increasing from room temperature to 200 °C, the tunable width is 0.114 μm.

From Fig. 1 (b), the GVM λ_f are 2.536, 2.579 and 2.650 μm at room temperature, 100 and 200 °C, leading to the corresponding QPM Λ of 35.62, 33.93 and 31.55 μm, respectively. Fig. 2 shows normalized SHG conversion efficiency η as a function of λ_f with the corresponding QPM Λ of GVM λ_f at room temperature, 100 and 200 °C for *o*+*e*-*e* type. With the small signal approximation, the normalized SHG conversion efficiency η is proportional to $\sin c^2(\Delta kL/2)$, where L is the crystal length. The SHG bandwidth is defined as the full width at half-maximum of the normalized SHG conversion efficiency η.[11] Bandwidths of o+e-e type QPM SHG are 88, 90 and 92 nm at room temperature, 100 and 200 °C, respectively.

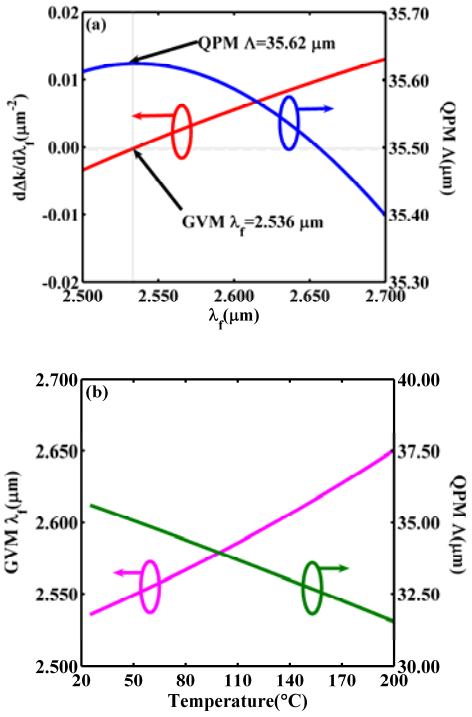

Fig. 1. The behaviors of o+e-e type QPM broadband SHG. (a) $\frac{d\Delta k}{d\lambda_f}$ *and QPM* Λ *as a function of* λ_f *at room temperature, (b) Dependence of temperature on GVM* λ_f *and corresponding QPM* Λ.

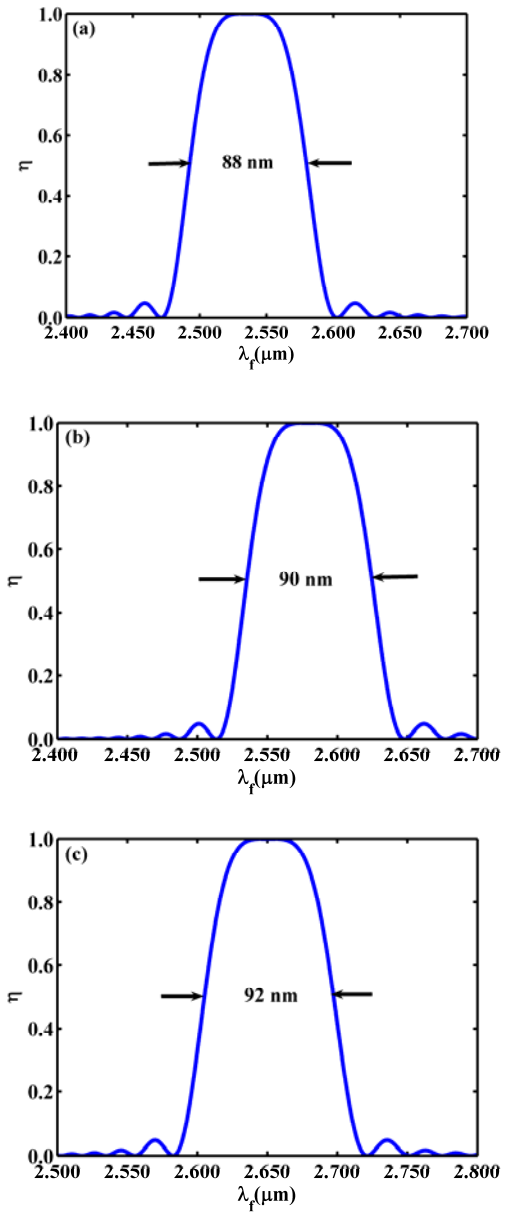

Fig. 2. Normalized SHG conversion efficiency η of o+e-e type QPM broadband SHG at (a) room temperature, (b) 100 and (c) 200 $^{\circ}C$.

For *o+o-o* type QPM, $\frac{d\Delta k}{d\lambda_f}$ and QPM Λ are calculated as a function of λ_f at room temperature, as shown in Fig. 3 (a). The GVM λ_f is 2.557 μm and corresponding QPM Λ is 34.11 μm. The dependence of temperature on GVM λ_f and corresponding QPM Λ is shown in Fig. 3 (b). The GVM λ_f increases from 2.557 to 2.575 μm and corresponding QPM Λ decreases from 34.11 to 33.98 μm with temperature increasing from room temperature to 200 $^{\circ}C$, the tunable width is 0.018 μm. Fig. 4 shows normalized SHG conversion efficiency η as a function of λ_f with the corresponding QPM Λ of GVM λ_f at room temperature, 100 and 200 $^{\circ}C$ for *o+o-o* type. The GVM λ_f are 2.557, 2.564 and 2.575 μm, corresponding QPM Λ are 34.11, 34.06 and 33.98 μm, and SHG bandwidths are 88, 89 and 89 nm at room temperature, 100 and 200 $^{\circ}C$, respectively.

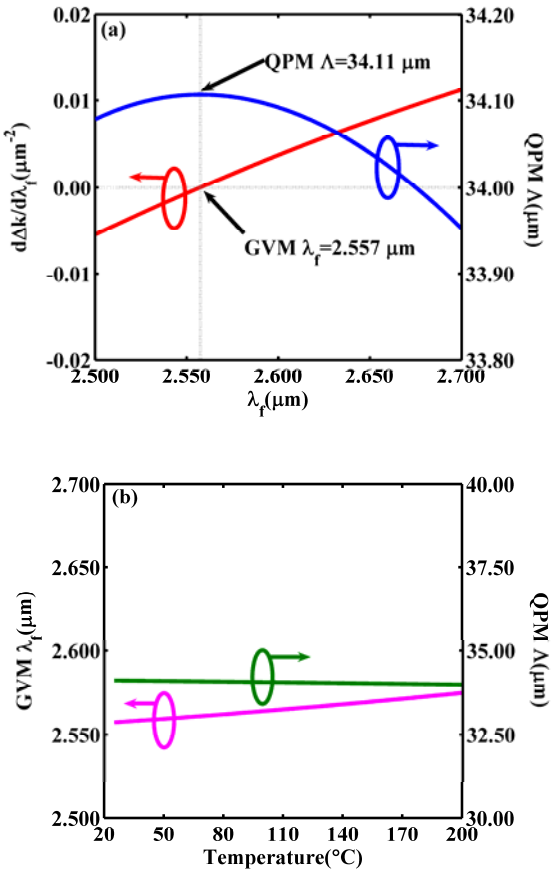

Fig. 3. The behaviors of o+o-o type QPM broadband SHG. (a) $\frac{d\Delta k}{d\lambda_f}$ and QPM Λ as a function of λ_f at room temperature, (b) Dependence of temperature on GVM λ_f and corresponding QPM Λ.

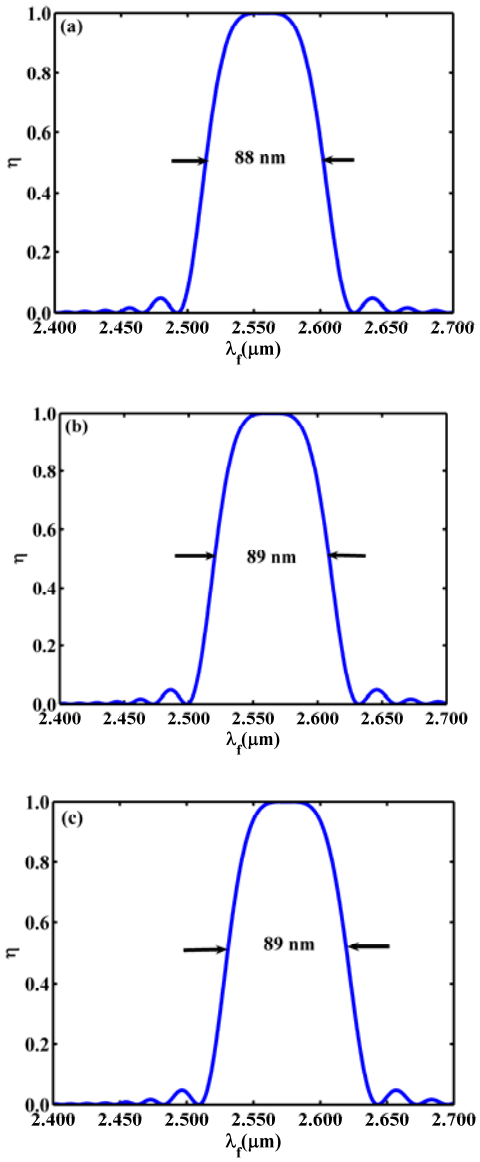

Fig. 4. Normalized SHG conversion efficiency η of o+o-o type QPM broadband SHG at (a) room temperature, (b) 100 and (c) 200 °C.

For *o+e-o* type QPM, $\frac{d\Delta k}{d\lambda_f}$ and QPM Λ are calculated as a function of λ_f at room temperature, as shown in Fig. 5 (a). The GVM λ_f is 2.597 μm and corresponding QPM Λ is 33.68 μm. The dependence of temperature on GVM λ_f and corresponding QPM Λ is shown in Fig. 5 (b). The GVM λ_f decreases from 2.597 to 2.515 μm and corresponding QPM Λ increases from 33.68 to 37.32 μm with temperature increasing from room temperature to 200 °C, the tunable width is -0.082 μm. Fig. 6 shows normalized SHG conversion efficiency η as a function of λ_f with the corresponding QPM Λ of GVM λ_f at room temperature, 100 and 200 °C for *o+e-o* type. The GVM λ_f are 2.597, 2.565 and 2.515 μm, corresponding QPM Λ are 33.68, 34.97 and 37.32 μm, and SHG bandwidths are 91, 89 and 86 nm at room temperature, 100 and 200 °C, respectively.

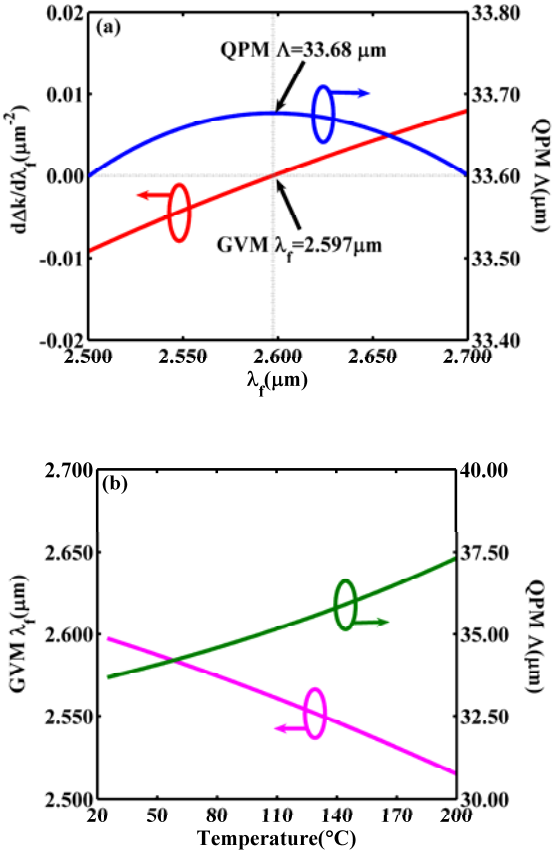

Fig. 5. The behaviors of o+e-o type QPM broadband SHG. (a) $\frac{d\Delta k}{d\lambda_f}$ and QPM Λ as a function of λ_f at room temperature, (b) Dependence of temperature on GVM λ_f and corresponding QPM Λ.

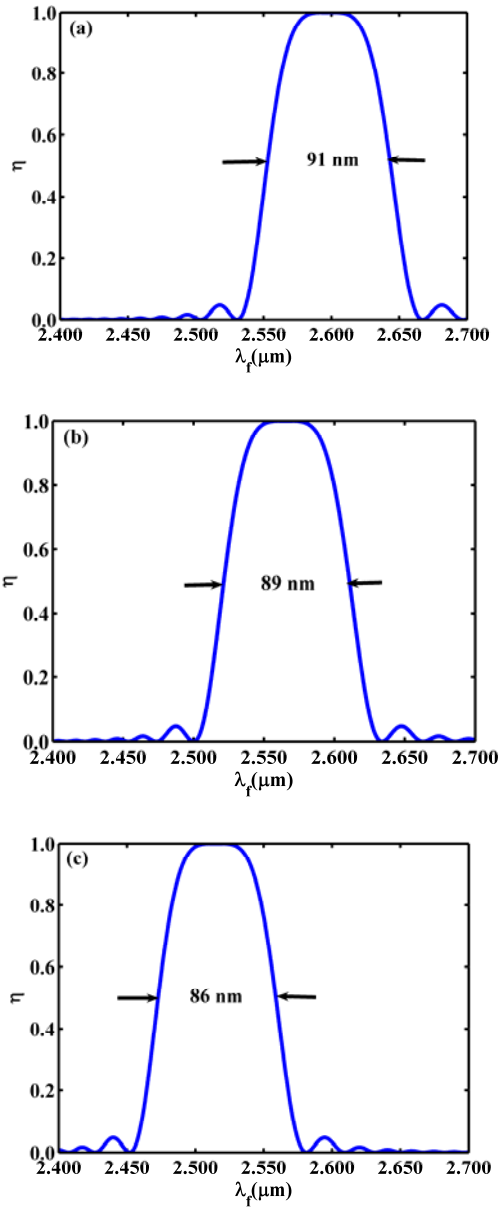

Fig. 6. Normalized SHG conversion efficiency η of o+e-o type QPM broadband SHG at (a) room temperature, (b) 100 and (c) 200 $^{\circ}C$.

For *e+e-o* type QPM, $\frac{d\Delta k}{d\lambda_f}$ and QPM Λ are calculated as a function of λ_f at room temperature, as shown in Fig. 7 (a). The GVM λ_f is 2.639 μm and corresponding QPM Λ is 33.28 μm. The dependence of temperature on GVM λ_f and corresponding QPM Λ is shown in Fig. 7 (b). The GVM λ_f decreases from 2.639 to 2.458 μm and corresponding QPM Λ increases from 33.28 to 41.49 μm with temperature increasing from room temperature to 200 $^{\circ}C$, the tunable width is -0.181 μm. Fig. 8 shows normalized SHG conversion efficiency η as a function of λ_f with the corresponding QPM Λ of GVM λ_f at room temperature, 100 and 200 $^{\circ}C$ for *e+e-o* type. The GVM λ_f are 2.639, 2.567 and 2.458 μm, corresponding QPM Λ are 33.28, 35.92 and 41.49 μm, and SHG bandwidths are 94, 89 and 83 nm at room temperature, 100 and 200 $^{\circ}C$, respectively.

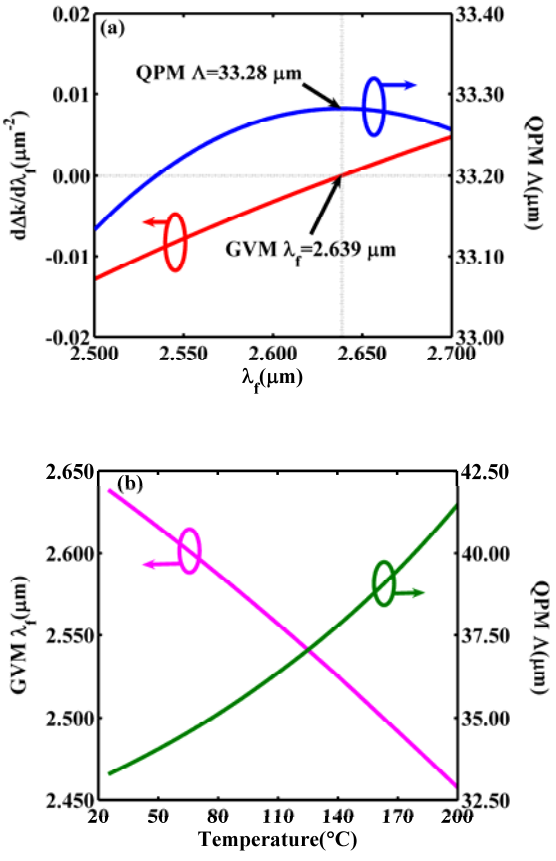

Fig. 7. The behaviors of e+e-o type QPM broadband SHG. (a) $\frac{d\Delta k}{d\lambda_f}$ and QPM Λ as a function of λ_f at room temperature, (b) Dependence of temperature on GVM λ_f and corresponding QPM Λ.

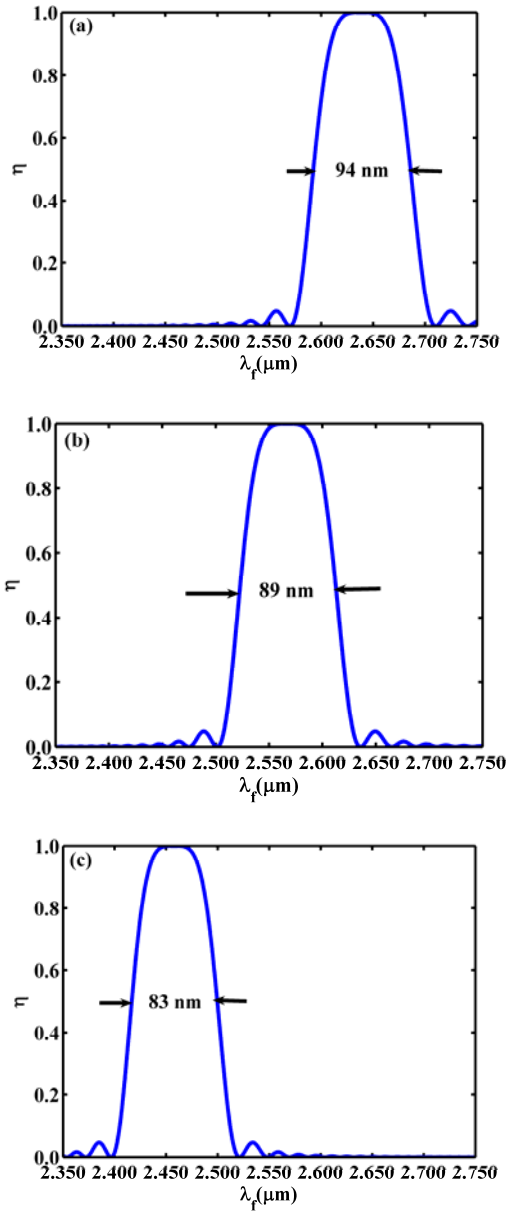

Fig. 8. Normalized SHG conversion efficiency η of e+e-o type QPM broadband SHG at (a) room temperature, (b) 100 and (c) and 200 °C.

4. Discussions

For a clear study of the effect of polarization on QPM broadband SHG in PPLT, a summary of some parameters for QPM broadband SHG is shown in Table 1. Results of *o+o-e* and *e+e-e* types are obtained in [13]. The GVM fundamental tunable range is the variation of GVM λ_f from room temperature to 200 °C. The temperature sensitivity of GVM λ_f is GVM fundamental tunable width divided by temperature variation. The minus of temperature sensitivity represents that GVM λ_f decreases with temperature increasing.

The six QPM types are usually divided into three categories. Type 0 includes *o+o-o* and *e+e-e* types, type Ⅰ includes *o+o-e* and *e+e-o* types, type Ⅱ includes *o+e-e* and *o+e-o* types.

From Table 1, one type Ⅰ interaction (*e+e-o* type) has the longest GVM λ_f and another type Ⅰ interaction (*o+o-e* type) has the shortest GVM λ_f at room temperature, however, *e+e-o* type interaction has the shortest GVM λ_f and *o+o-e* type interaction has the longest GVM λ_f at 200 °C. The GVM λ_f is positively correlated with temperature for *o+o-e*, *o+e-e*, *o+o-o* and *e+e-e* types, and the GVM λ_f is negatively correlated with temperature for *o+e-o* and *e+e-o* types. The temperature sensitivity of GVM λ_f for type Ⅰ interaction is maximum and that for type 0 interaction is minimum, type Ⅱ has the moderate one.

The effect of polarization on SHG bandwidth shows similar tendencies to GVM λ_f. The SHG bandwidth increases with temperature increasing for *o+o-e*, *o+e-e* and *o+o-o* types, The SHG bandwidth decreases with temperature increasing for *e+e-e*, *o+e-o* and *e+e-o* types. The type Ⅰ interaction has the maximum bandwidth variation range, type 0 interaction has the minimum bandwidth variation range, type Ⅰ interaction has the moderate one.

The GVM condition is fulfilled by wavelength and refractive indices balance. Refractive indices of different polarization waves are not the same at the same wavelength. So when QPM type changes, the original balance is break with polarization varying, the new balance is established by wavelength changing. Refractive index depends on not only wavelength but also temperature. Effects of temperature on refractive index are different for different polarization waves, different QPM types are combinations of different polarization lights, so effects of temperature on GVM λ_f and SHG bandwidth are different for different QPM types.

In Z-cut PPLT, assuming that the fundamental and second-harmonic beams propagate along the x-axis of the crystal, the effective nonlinear coefficient d_{eff} for six types are calculated, d_{eff} are d_{31}, 0, d_{22}, d_{33}, d_{31} and 0 for *o+o-e*, *o+e-e*, *o+o-o*, *e+e-e*, *o+e-o* and *e+e-o* types, respectively. The values of nonlinear coefficients ($d_{33}=16$, $d_{22}=1.7$, $d_{31}=1$ pm/V) are given in [19].

For first-order QPM, the QPM effective nonlinear coefficient d_Q can be described as [20]

$$d_Q = d_{eff}\frac{2}{\pi}, \tag{8}$$

the non-normalized conversion efficiency η' is as shown [20]

$$\eta' \propto \left(d_Q\right)^2 \times \mathrm{sinc}^2(\Delta kL/2). \tag{9}$$

Table 1. Summary of some parameters for QPM broadband SHG in PPLT

	GVM fundamental tunable range (μm)	Temperature sensitivity (nm/°C)	Bandwidth at room temperature (nm)	Bandwidth at 100 °C (nm)	Bandwidth at 200 °C (nm)
o+o-e	2.497-2.712	1.229	85	89	96
o+e-e	2.536-2.650	0.651	88	90	92
o+o-o	2.557-2.575	0.103	88	89	89
e+e-e	2.575-2.590	0.086	90	89	89
o+e-o	2.597-2.515	-0.469	91	89	86
e+e-o	2.639-2.458	-1.034	94	89	83

So SHG conversion efficiencies for *o+o-e*, *o+o-o* and *o+e-o* QPM types would be reduced to $(d_{31}/d_{33})^2$=0.004 , $(d_{22}/d_{33})^2$=0.011 and $(d_{31}/d_{33})^2$=0.004 in reference to the *e+e-e* QPM type, respectively. However, some applications' requirements are not only conversion efficiency but wavelength and temperature sensitivity. For example, d_{31} is less than d_{33} in PPLN, but *o+o-e* QPM type is widely used in all optical wavelength conversion for its fundamental wavelength.

In Z-cut PPLT, assuming that the fundamental and second-harmonic beams propagate along the x-axis of the crystal, SHG can not be achieved for *o+e-e* and *e+e-o* QPM types. However, in many other cutting and propagating styles, the effective nonlinear coefficients of these two QPM types do not equal zero, SHG can be achieved for *o+e-e* and *e+e-o* QPM types. So discussion of *o+e-e* and *e+e-o* QPM types is meaningful.

Polarization is an influencing factor of QPM broadband SHG like temperature [13] and magnesium oxide doping concentration [15]. Results show effects of polarization on GVM λ_f and SHG bandwidth, and GVM λ_f and SHG bandwidth variations with temperature. Some new wavelength QPM broadband SHGs can be obtained by changing polarizations of fundamental and second-harmonic waves. The QPM type can be chosen to obtain suitable temperature sensitivity in temperature-varying condition.

5. Conclusions

In conclusion, polarization is an influencing factor of QPM broadband SHG in PPLT. GVM fundamental wavelength and SHG bandwidth vary with polarizations of fundamental and second-harmonic waves varying. GVM fundamental wavelength and SHG bandwidth are positively correlated with temperature for some QPM types and negatively for another QPM types. The temperature sensitivity of GVM fundamental wavelength for type Ⅰ interaction is maximum and that for type 0 interaction is minimum. These results can be used in designs of new wavelength QPM broadband SHG.

Acknowledgements

This work is supported by the National Natural Science Foundation of China (Grant Nos. 11647094, 41574137 and 41574136), Science and Technology Innovation Seedling Project of Sichuan Province (Grant No. 2016038), Young and Middle-aged Key Teacher Training Program of Chengdu University of Technology, and Excellent Innovation Team Development Program of Chengdu University of Technology.

References

[1] W. Dang, Y. Chen, M. Gong, X. Chen, Appl. Phys. B-Lasers Opt. **110**(4), 477 (2013).
[2] Z. Huang, C. Tu, S. Zhang, Y. Li, F. Lu, Y. Fan, E. Li, Opt. Lett. **35**(6), 877 (2010).
[3] N. E. Yu, S. Kurimura, K. Kitamura, O. Jeon, M. Cha, S. Ashihara, T. Ohta, T. Shimura, K. Kuroda, J. Hirohashi, Appl. Phys. Lett. **85**(24), 5839 (2004).
[4] S. H. Bae, I. H. Beak, S. Y. Choi, W. B. Cho, F. Rotermund, C. S. Yonn, Opt. Commun. **283**(9), 1894 (2010).
[5] F. Konig, F. N. C. Wong, Appl. Phys. Lett. **84**(10), 1644 (2004).
[6] R. Wu, Y. Chen, J. Zhang, X. Chen, Y. Xia, Appl. Optics **44**(26), 5561 (2005).
[7] F. Laurell, T. Calmano, S Muller, P. Zeil, C. Canalias, G. Huber, Opt. Express **20**(20), 22308 (2012).

[8] N. E. Yu, J. H. Ro, M. Cha, S. Kurimura, T. Taira, Opt. Lett. **27**(12), 1046 (2002).
[9] N. E. Yu, S. Kurimura, K. Kitamura, J. H. Ro, M. Cha, S. Ashihara, T. Shimura, K. Kuroda, T. Taira, Appl. Phys. Lett. **82**(20), 3388 (2003).
[10] M. Yin, S. Zhou, G. Feng, Acta Phys. Sin. **61**(23), 234206 (2012).
[11] J. Zhang, Y. Chen, F. Lu, W. Lu, W. Dang, X. Chen, Y. Xia, Appl. Optics **46**(32), 7791 (2007).
[12] S. Ashihara, T. Shimura, K. Kuroda, J. Opt. Soc. Am. B **20**(5), 853 (2003).
[13] M. Yin, J. Korean Phys. Soc. **67**(10), 1750 (2015).
[14] S. Stivala, A. C. Busacca, A. Pasquazi, R. L. Oliveri, R. Morandotti, G. Assanto, Opt. Lett. **35**(3), 363 (2010).
[15] X. Zhong, M. Yin, M. Lian, J. Optoelectron. Adv. M. **18**(7-8), 613 (2016).
[16] K. Lee, C. S. Yoon, F. Rotermund, Jpn. J. Appl. Phys. **44**(3), 1264 (2005).
[17] M. Yin, J. Optoelectron. Adv. M. **17**(9-10), 1253 (2015).
[18] I. Dolev, A. Padowicz, O. Gayer, A. Arie, J. Mangin, G. Gadret, Appl. Phys. B-Lasers Opt. **96**(2-3), 423 (2009).
[19] W. Martienssen, H. Warlimont, "Handbook of Condensed Matter and Materials Data", Springer, Berlin, pp. 849, 2005, 1st ed.
[20] Y. Chen, X. Chen, S. Xie, X. Zeng, Y. Xia, Y. Chen, J. Opt. A-Pure Appl. Opt. **4**(3), 324 (2002).

*Corresponding author: yinmingcdut@163.com